Eur. Phys. J. B **43**, 509–515 (2005)
DOI: 10.1140/epjb/e2005-00084-8

THE EUROPEAN PHYSICAL JOURNAL B

Magnetism of mixed valence (LaSr) hexaferrites

P. Novák[1,a], K. Knížek[1], M. Küpferling[2], R. Grössinger[2], and M.W. Pieper[2]

[1] Institute of Physics of ASCR, Cukrovarnická 10, 162 53 Prague 6, Czech Republic
[2] Institute for Solid State Physics, Technical University Vienna, Wiedner Hauptstrasse 8-10, 1040 Vienna, Austria

Received 27 August 2004 / Received in final form 18 January 2005
Published online 30 March 2005 –

Abstract. The electronic structure of $La_xSr_{1-x}Fe_{12}O_{19}$ ($x = 0$, 0.25, 0.5, 0.75, 1) hexaferrite is calculated using the density functional theory and generalized gradient approximation (GGA). The GGA+U method is used to improve the description of strongly correlated $3d$ electrons of Fe. The 'virtual crystal' approach is employed for the fractional x, its applicability is checked for $x = 0.5$ by comparing it with the supercell method. The electronic charges introduced by the La substitution show no significant preference for any of the iron sublattices. The magnetic moment decreases linearly with the increasing La content in agreement with the experiment.

PACS. 75.50.Gg Ferrimagnetics – 71.28.+d Narrow band systems, intermediate valence solids

1 Introduction

M-type hexaferrites play an important role at the permanent magnet market since several decades because of their low cost and chemical stability. Even slight improvements in magnetic properties would be of great importance for industrial application, which was the reason for a large and continuous interest in improvements of the theoretical description and in attempts to tune the magnetic properties by substituting elements at various lattice sites [1]. A typical representant of the M-type hexaferrites is $SrFe_{12}O_{19}$ and its crystal structure is displayed in Figure 1. Already in 1974 a substitution with La was found to be interesting, due to a remarkably high anisotropy at low temperatures discovered in $LaFe_{12}O_{19}$ [2]. The increase in anisotropy field was attributed to a change from Fe^{3+} to Fe^{2+} on the 2a-Fe sublattice. This explained the smaller magnetization and made plausible a contribution to the anisotropy constant from an unquenched orbital momentum of Fe^{2+}.

Renewed interest from industry in the problem triggered some recent experimental work at intermediate concentrations x but despite the fact that the ionic radii of La^{3+} and Sr^{2+} ions are very close, 0.115 and 0.113 nm, respectively, mixed valence hexaferrites $La_xSr_{1-x}Fe_{12}O_{19}$ are very difficult to prepare. As the $LaFe_{12}O_{19}$ phase seems to be a high temperature phase (temperature range of stability between 1380 °C and 1420 °C [3]), it dissociates easily into $LaFeO_3$ and Fe_2O_3, which can only be prevented by rapid quenching from a temperature within the stability range down to room temperature. Mixed hexaferrites of the form $RE_xSr_{1-x}Fe_{12}O_{19}$ (RE=La, Sm, Nd, Pr) with $x > 1/3$ seem to be unstable at room temperature [4] and for concentrations $0 < x < 1/3$ the amount of RE ions that really enters the hexaferrite lattice structure has still to be investigated. There are, therefore, no experimental investigations since the early works of Lotgering and Sauer et al. [2,5] to support the empirical model for the increased magnetic anisotropy in the La-hexaferrite.

A more detailed analysis of the anisotropy mechanism should be based on a realistic ab initio band structure calculation, which was impossible at that time. The electronic structure of the stoichiometric strontium hexaferrite was calculated recently by Fang et al. [6]. These authors used the localized spherical wave method (LSW) employing density functional theory (DFT) and the local spin density approximation (LSDA). In the LSW method the crystal is divided into overlapping atomic spheres. Several different spin structures were considered and the experimentally observed stable structure (denoted as Gorter structure [7]) with spins on 2a, 2b and 12k sites antiparallel to spins on $4f_1$ and $4f_2$ sites was found to have the lowest total energy. The resulting electronic structure corresponds to an insulator, again in agreement with experiment. Note that here are two dangers when applying the LSW method to the hexaferrite structure: First, LSW is not a full potential method as the potential is spherically averaged within the atomic spheres. It is, therefore, also not well suited to calculate the magnetic anisotropy. Second, to fill the space in the relatively loosely packed hexaferrite structure, 'empty atomic spheres' must be added in a rather arbitrary procedure.

In order to improve this we performed calculations of the electronic structure of M-type hexaferrite employing the WIEN2k program [8]. This program is based on the density functional theory and it uses the full-potential linearized augmented plane wave (FPLAPW) method with the dual basis set. To study the influence of

[a] e-mail: novakp@fzu.cz

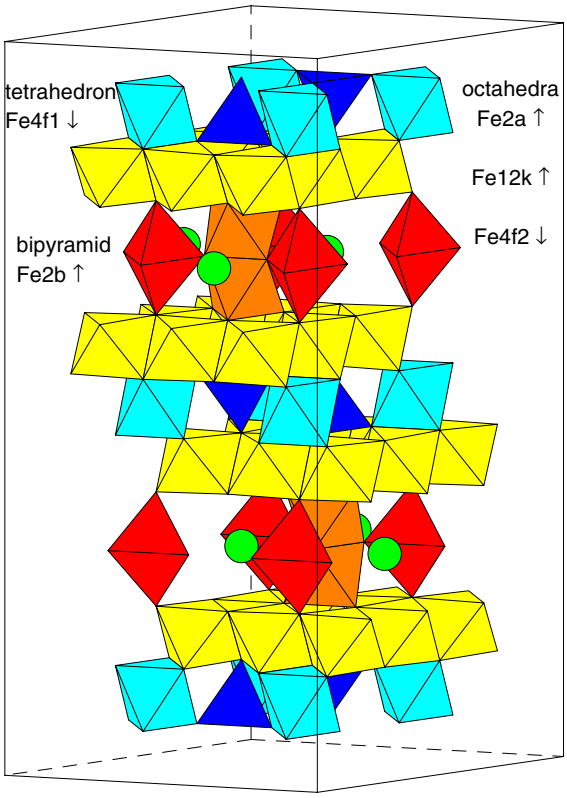

Fig. 1. Structure of $SrFe_{12}O_{19}$. The topmost layer consists of 2a-Fe octahedra (light color) and $4f_1$-Fe tetrahedra (dark color). The second layer consists of 12k-Fe octahedra. The third layer consists of $4f_2$-Fe octahedra (light color) and 2b-Fe bipyramids (dark color). The arrows attached to the site label indicate the spin orientation for respective sites. The spheres correspond to Sr atoms.

carrier doping we extended the calculations to mixed valence $La_xSr_{1-x}Fe_{12}O_{19}$ compounds. All calculations were performed with the Gorter spin structure and identical crystal structure parameters [9,10].

Our main goal was to find out how electronic structure and magnetism of $La_xSr_{1-x}Fe_{12}O_{19}$ develop when the lanthanum concentration increases. Particular emphasis was placed on the analysis of the results with respect to the contributions of different sublattices to the charge and spin densities. In this way we can estimate the viability of ab initio calculations of the empirical mechanism proposed for the magnetocrystalline anisotropy. Actual calculations of the orbital momentum, magnetocrystalline anisotropy and the hyperfine parameters will be considered in a separate paper.

2 Calculation method

In the APW-like methods the space is divided into nonoverlapping atomic spheres and the interstitial region. The electron states are then classified into core states which are fully contained in the atomic spheres, and valence states. The valence states are expanded using atomic-like basis functions in the spheres augmented by plane waves in the interstitial region. So called local orbitals are added to these basis functions to treat two valence functions with the same orbital number (like $3p$ and $4p$ functions of Fe) [11]. In our calculations the electronic configuration of the core states corresponded to (Ne, $3s^2$) for Fe, to He for O, to (Ar, $3d^{10}$) for Sr and to (Kr, $4d^{10}$) for La atoms. The radii of the atomic spheres were 2.00 for La and Sr, 1.9 for all five inequivalent Fe and 1.6 a.u. for the oxygens. The leakage of the core states can be safely neglected so the outer ten (eleven) electrons of Sr (La) are placed on valence states which differ only in their main quantum number. They are responsible for the change of the density as the La concentration is increased. We emphasize that charge or spin counts on individual atoms that are discussed below refer to this division of space, i.e. the values depend to some extent on the size of the atomic spheres.

The number n_k of the k points in the irreducible part of the Brillouin zone was 4. The calculations were converged with a rather small number of basis functions per atom in the unit cell ($Rk_{max} = 4.2$, $n_b \approx 37$), n_b was then increased to ≈66 ($Rk_{max} = 5.8$) and the calculation run to full convergence. The results obtained with these two n_b differed only slightly. Increasing n_k from 4 to 7 had a small effect too – the effect of La-doping on the local magnetic moment of iron discussed below is an order of magnitude larger.

All calculations were spin-polarized, assuming the Gorter ferrimagnetic ordering of the Fe spins. For the exchange correlation potential we adopted the GGA form [12] as for the $3d$ compounds it is superior to the LSDA, as a rule. A calculation with the LSDA exchange-correlation potential [13] was performed for the stoichiometric strontium ferrite in order to compare the results with those in reference [6].

2.1 GGA+U

Despite the fact that in many cases GGA gives better results than LSDA when applied to systems with $3d$ electrons, in the $3d$ transition metal oxides the energy gap and the magnetic moment are still underestimated [14]. To improve the description of Fe $3d$ electrons we thus used the rotationally invariant version of the LDA+U method as described by Liechtenstein et al. [15], but with the GGA instead of LSDA exchange-correlation potential. The method should be therefore more correctly denoted as GGA+U. The method is no longer truly ab initio as the values of the Hubbard parameter U and the exchange parameter J must be inserted. These can either be taken from the experiment or estimated using the restricted LSDA (GGA) calculation. The restricted LSDA calculation [16] of $LaFeO_3$ yielded the values $U = 7.7$ and 9.3 eV for ferrous and ferric ion, respectively. A smaller value $U(Fe^{3+}) = 5.5$ eV was deduced from the photoemission and inverse photoemission experiments on α-Fe_2O_3 [17]. The exchange parameter J is believed to be close to its atomic value $J \sim 1$ eV [16]. In any case we can rely on

reasonable limits for these parameters rather than on their specific values (this concerns especially U).

In the LDA+U methods an orbitally dependent potential is introduced for the chosen set of electron states, which in our case are $3d$ states of Fe. The additional potential has an atomic Hartree-Fock form, but with screened Coulomb and exchange interaction parameters. The problem is that the exchange and correlation already contained in the LSDA or GGA should be subtracted. The form of this 'double counting correction' is spherically symmetrical and it is not clear to which extent its application in the full potential methods is justified, as there is no 'double counting correction' for the nonspherical terms in the orbital potential. We avoided this problem by using an effective $U_{eff} = U - J$ instead of the parameter U, and putting the nonspherical terms in the orbital potential equal to zero. In what follows the notation $U \equiv U_{eff}$ is used, but it should be kept in mind that we are dealing with the effective U which is somewhat smaller than the Hubbard parameter as $J/U \approx 0.1 - 0.2$. To see how the results depend on U, two values $U = 3.4$ and 6.9 eV were employed in addition to the GGA calculation which corresponds to $U = 0$.

2.2 Mixed valence region

In the mixed valence region the distribution of the La^{3+} ions is presumably random. In this situation, in order to treat the substitution, the supercell method is usually used. However, in the present spin-polarized calculations the unit cell of the parent compound comprises two formula units, or 64 atoms, eleven of which are inequivalent. To perform the supercell calculation with the FPLAPW method would then be costly and for x close to zero or one near to impossible. To overcome this difficulty, we used the fact that the valence electron functions for La and Sr are very similar (the chemical bonding is very similar). The substitution can then be treated by a 'virtual crystal' method, successfully applied to $3d$ mixed valence oxides earlier [18,19]. In the 'virtual crystal' method the electrons, the number of which is equal to the number of La atoms, are introduced by increasing the number of valence electrons per unit cell by $N_u x$, where $N_u = 2$ is the number of formula units in the unit cell. To keep the system electrically neutral the Sr atoms with atomic number $Z = 38$ are replaced by 'virtual' atoms with fractional atomic number $Z = 38 + x$. The system retains original periodicity, so that any effect of the disorder is suppressed.

To check the applicability of the method we performed for $La_{0.5}Sr_{0.5}Fe_{12}O_{19}$ three calculations – in the first one virtual atoms with $Z = 38.5$ were introduced instead of all Sr atoms, in the second virtual atoms with $Z = 56.5$ replaced all La atoms ($Z = 57$), and in the third calculation one of the two Sr in the unit cell was replaced by La (GGA exchange correlation potential was employed). As seen in Table 1 the calculations yielded very similar results – e.g. the Fe spins change by less than 1% and there is negligible change in the density of states near the Fermi energy. We conclude therefore that if the effect of disorder can be neglected, the substitution of strontium by lanthanum is well accounted for by the 'virtual crystal' method and we employed this method to obtain the results described below.

Table 1. $La_{0.5}Sr_{0.5}Fe_{12}O_{19}$, GGA calculation. Magnetic moments of iron atoms calculated by virtual crystal method with virtual Sr atom (denoted VA Sr), La atom (denoted VA La) and in a standard way with one Sr and one La atom in the unit cell (denoted Sr, La). In the last method the symmetry is reduced and the number of inequivalent sites increases from five to nine (all sublattices except 2a are split in two). The total magnetic moment of the unit cell that includes moments on all atoms and in the interstitial is also given. All moments are in μ_B.

site	VA Sr	VA La	Sr, La
2a	3.656	3.658	3.657
2b(1)	3.468	3.459	3.440
2b(2)	3.468	3.459	3.464
$4f_1(1)$	–3.378	–3.379	–3.378
$4f_1(2)$	–3.378	–3.379	–3.376
$4f_2(1)$	–3.319	–3.313	–3.337
$4f_2(2)$	–3.319	–3.313	–3.274
12k(1)	3.649	3.648	3.668
12k(2)	3.649	3.648	3.624
total	39.008	39.009	39.006

3 Results

3.1 Stoichiometric strontium hexaferrite

The calculated electronic structure of $SrFe_{12}O_{19}$ corresponds to a metal when LSDA is used with the FPLAPW approach (Fig. 2, bottom), there is a finite DOS at the Fermi energy E_F in the majority as well as in the minority spin channel. We note that a Gaussian broadening 0.003 Ry was used to smooth DOS in this case, as well as in all cases described below. The material is on the border between metal and semiconductor if GGA is used for the exchange potential which enlarges the gap in both spin channels almost to the size that it overlaps. An insulator results only with a non-vanishing on-site repulsion parameter U. The band structure for GGA+U has a gap of ≈1.2 eV for $U = 3.4$ eV that increases to ≈2.1 eV as U is increased to 6.9 eV. In Figure 2 the total densities of states (DOS) obtained in these four calculations are displayed.

The states close to the Fermi energy E_F have predominantly $3d$ Fe character with some oxygen $2p$ mixing in the LSDA and GGA calculations. The oxygen character prevails when the GGA+U is applied. The DOS projected on the $3d$ states of the five inequivalent iron ions are shown in Figure 3 together with the sum of the oxygen DOS. Note that the empty states of the projected DOS in this ferrimagnetic structure appear in the (global) minority spin channel only for 2a-, 2b-, and 12k-Fe sites, while they are in the majority spin channel for $4f_1$- and $4f_2$-Fe sites.

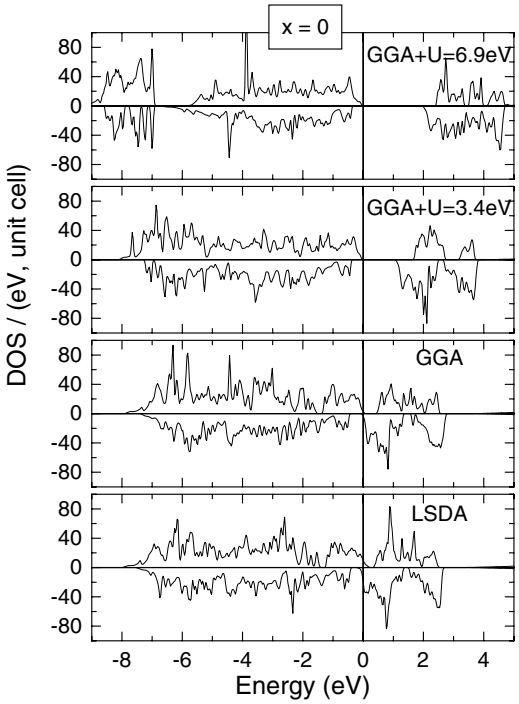

Fig. 2. Total DOS for majority (positive) and minority (negative) states in $SrFe_{12}O_{19}$ calculated by LSDA, GGA and GGA+U methods with $U = 3.4$ eV and $U = 6.9$ eV.

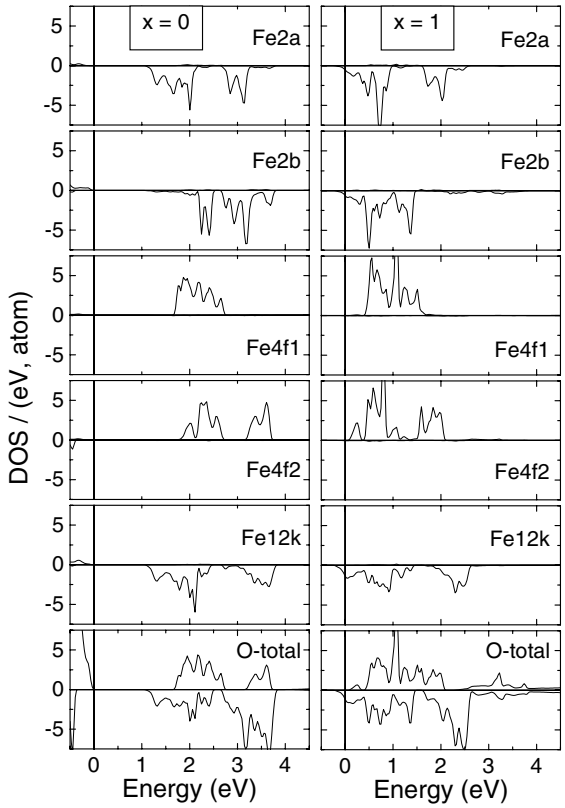

Fig. 3. DOS projected on the 3*d* states of five inequivalent iron ions calculated by GGA+U for $U = 3.4$ eV. The DOS corresponding to an averaged oxygen site is also shown. Left panel: $SrFe_{12}O_{19}$, right panel: $LaFe_{12}O_{19}$.

Table 2. Magnetic moments of the interstitial region and inequivalent atoms in $SrFe_{12}O_{19}$ calculated by LSDA, GGA and GGA+U methods. The total magnetic moment of the unit cell is also given. All moments are in μ_B.

atom	LSDA	GGA	GGA+U $U = 3.4$ eV	GGA+U $U = 6.9$ eV
Sr	0	0	0	0
Fe(2a)	3.51	3.68	4.01	4.20
Fe(2b)	3.35	3.47	3.88	4.12
$Fe(4f_1)$	–3.22	–3.37	–3.85	–4.11
$Fe(4f_2)$	–3.06	–3.33	–3.95	–4.18
Fe(12k)	3.50	3.69	4.02	4.21
O(4e)	0.34	0.37	0.33	0.27
O(4f)	0.10	0.11	0.08	0.06
O(6h)	0.08	0.06	0.03	0.02
$O(12k_1)$	0.08	0.09	0.08	0.06
$O(12k_2)$	0.17	0.18	0.16	0.13
interst.	2.64	2.77	2.49	2.29
total	38.48	39.91	40.01	40.01

Magnetic moments of all eleven inequivalent atoms and of the interstitial region of the stoichiometric strontium hexaferrite calculated by different methods are given in Table 2. In the insulating cases the sum of 40 μ_B per unit cell corresponds to 5 μ_B/Fe in the ferrimagnetic structure.

3.2 Lanthanum containing Sr hexaferrites

The electronic structure of $La_xSr_{1-x}Fe_{12}O_{19}$ in the mixed valence regime ($x = 0.25$, 0.5, 0.75 and 1) was calculated using GGA and GGA+U methods. The virtual crystal concept with Sr as the virtual atom was used for $x = 0.25$ and 0.5, while for $x = 0.75$ La virtual atom was introduced. Figure 4 shows resulting total DOS for $U = 3.4$ eV.

The nonintegral number of electrons n in the virtual crystal approach ($x = 0.25$ and 0.75) implies nonzero density of states at the Fermi energy while for integral n a gap may appear. In all cases we considered, the density of the majority spin (spin up) states exhibited a gap, while the DOS of the minority, spin down, states is nonzero at E_F. The electronic structure thus corresponds to a halfmetal with the conduction in the spin down channel only. The halfmetallic character of the system has a rather simple consequence for the dependence of total magnetic moment on the La concentration x: As explained in Section 2 B the number of valence electrons per unit cell is $n(x) = n(0) + 2x$. At the same time n is the sum of numbers of majority and minority spin electrons: $n = n_\uparrow + n_\downarrow$. Because of the gap, $n_\uparrow$ is an integer that does not depend on x (in principle it may change by an integer, but that was not found in the results of calculation). The total magnetic moment m_{tot} is then:

$$m_{tot}(x) = n_\uparrow(x) - n_\downarrow(x) = n_\uparrow(0) - [n(0) - n_\uparrow(0) + 2x] = m_{tot}(0) - 2x \quad (1)$$

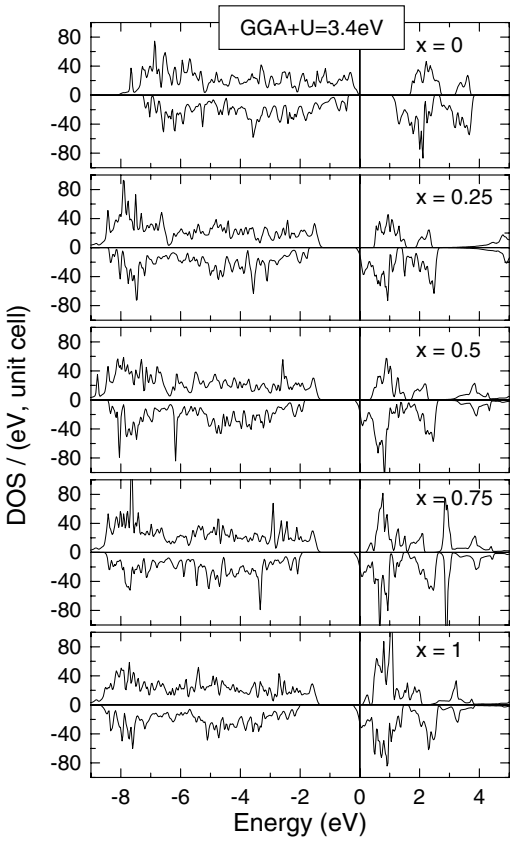

Fig. 4. Total density of states of $La_xSr_{1-x}Fe_{12}O_{19}$ calculated by GGA+U ($U = 3.4$ eV) as a function of the La concentration.

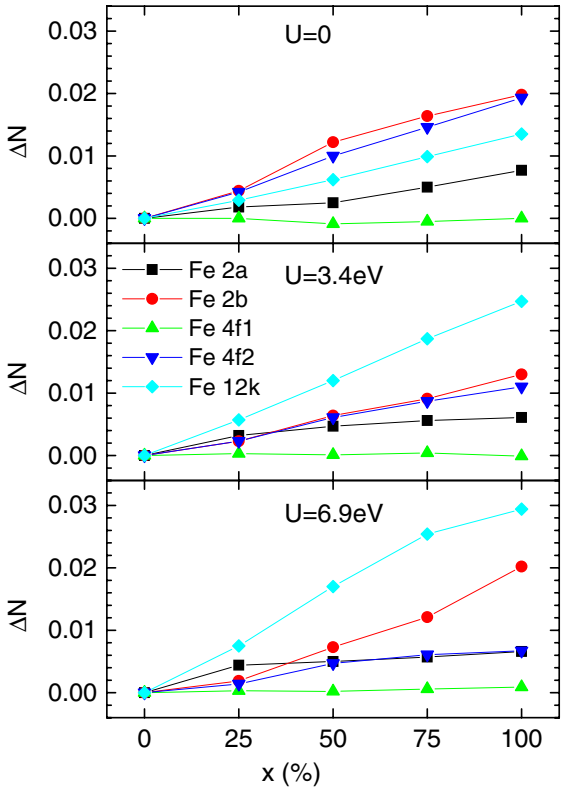

Fig. 5. Difference of the number of electrons per atom $\Delta N = N(x) - N(0)$ for the five inequivalent Fe sites as function of the La concentration for the GGA (upper panel), GGA+U, $U = 3.4$ eV (middle panel) and $U = 6.9$ eV (lower panel) calculations.

4 Discussion

Besides the fact that the present (full potential) LSDA calculation for $SrFe_{12}O_{19}$ resulted in a metallic state, instead of the insulator found by Fang et al. [6], the differences in the calculated DOS are rather small. Clearly the Gorter spin structure would prove energetically favorable within the FPLAPW approach as well. We note in passing that the use of the muffin-tin potential in the LSW method seems to compensate for the underestimation of correlation effects in LSDA.

The crystal field splitting of the t_{2g}- and e_g-states on the octahedral Fe-sites (2a, 12k, and $4f_2$) is clearly observed in the empty states. At $U = 3.4$ eV we find for the splitting, determined as the energy difference of the center of gravity of the partial t_{2g}- and e_g-DOS, 1.61, 1.31, and 1.18 eV for the 12k-, 2a-, and $4f_2$-sites, respectively. For the tetrahedral co-ordination the t_{2g}-e_g splitting is expected to be smaller compared to the splitting on the octahedral sites. This is indeed reflected in the Fe(f_1) DOS – there is no gap dividing these states.

When La is substituted for Sr extra valence electrons appear in the system. As described in the Introduction, the empirical explanation of the large magnetic anisotropy of La-hexaferrite hinges on a preference of these electrons for the 2a-Fe sublattice. A direct information on site preferences in real space is provided by the number N_i of electrons in the atomic sphere i. This must be taken with a caution, however, as any such division reflects the real situation only approximately, in particular N_i depend on the chosen atomic radii. Nevertheless, taking the same reasonable value 1.9 a.u. for the radius of all five inequivalent irons, we believe that a good estimation for the preference is obtained. The difference $\Delta N_i = N_i(x) - N_i(0)$ for the five inequivalent Fe-sites is plotted in Figure 5 for $U = 0$, 3.4 and 6.9 eV.

First of all it is seen that most of the additional electrons are, in fact, not contained in atomic spheres of Fe, the total count at $x = 1$ accounts for only 0.38 electrons per unit cell. The fact that most of the additional electrons end up in the interstitial regime indicates already that no significant site preferences are predicted. In addition, a small but finite DOS at E_F is predicted for $x = 1$. This corresponds well to preliminary measurements showing that the resistivity of $LaFe_{12}O_{19}$ at room temperature is several orders of magnitude smaller than that of $SrFe_{12}O_{19}$ [20], and to NMR investigations at small x showing the presence of an internal field which appears to be very homogeneous since it is the same size at all Fe-sites [21].

In more detail, the behavior of the 2a-, 2b-, and $4f_1$-sites is predicted fairly independent of the special value of U: No additional charges enter the sphere at $4f_1$-Fe, and at 2a-Fe the charge difference stays below 1% in all cases.

The 2b-Fe sublattice is predicted to take app. twice as much electrons at $x = 1$, but due to the small multiplicity this still is a small percentage of the total count. However, it is also seen that the calculated distribution of the doped electrons in the unit cell does depend significantly on the parameter U for the 12k- and $4f_2$-sublattices. With increasing U ΔN_{12k} increases, while ΔN_{4f2} decreases at all x.

This may indicate an oversimplification in the calculations: We used the same on-site repulsion for all Fe sites while in reality U depends on coordination and bonding. Preferably one should determine U separately for all five inequivalent sites. Due to the complexity of the structure such calculations are outside the scope of the present work. We note, however, that calculations of U in magnetite Fe_3O_4 [22] showed differences as large as 1 eV within one structure. To check for the influence of such a difference in the local U we performed the GGA+U calculation at $x = 1$ with $U = 5.7$ eV for the 2a-site while it was kept at $U = 6.9$ eV for all other Fe-sublattices. As expected, the smaller on-site repulsion increases the electron content of the atomic sphere at 2a-Fe, in this case by 0.04 electrons. This indicates that the absolute effect of site specific parameters U will be small, but inspection of Figure 5 shows that the influence on the relative amount of additional charge at the five sites might be considerable.

In the LDA+U-like methods the energy of occupied states is lowered, while the energy of unoccupied states increases. As a consequence more solutions of the self-consistent procedure may be obtained, depending on the starting occupation matrix. To check whether we might have missed in this way a solution with strong localization at 2*a*-sites as proposed from the experimental point of view [2] we performed a calculation in which the starting population matrices corresponded to this situation. After several scf loops the electron was smeared over different sites, however, and the converged result was identical with the one obtained before. We conclude therefore that the solution with the delocalized electron is a robust one. Note, however, that in the 'virtual crystal' approach the disorder is disregarded. As a consequence we cannot rule out that (especially for small x) the disorder may cause the localization. In this connection it would be clearly desirable to use the CPA method [23] that, unfortunately, is not implemented in the WIEN2k program.

In the above analysis the charge of a given iron atom was calculated by integrating the electron density contained in corresponding atomic sphere. This method is simple, but it reflects the true atomic charge only qualitatively. To substantiate the analysis the crystal charge was decomposed also using the 'Atoms in Molecules' (AIM) method [24]. AIM divides the crystal electron density among the atoms without introducing the spheres and it is probably the best method available at present. AIM method requires, however, a lot of computer time and we thus calculated the AIM charges for $x = 0$, 1 and $U = 3.4$ eV only. As seen from Table 3 the conclusion that there is no clean-cut preference for the extra charge holds also when AIM is used.

Table 3. Comparison of 'Atoms in Molecules' (AIM) and conventional (AS) methods. ΔN is the difference between the numbers of electrons per atom in $LaFe_{12}O_{19}$ and in $SrFe_{12}O_{19}$. GGA+U method with $U = 3.4$ eV was used.

site	ΔN(AS)	ΔN(AIM)
2a	0.006	0.012
2b	0.013	0.030
$4f_1$	0.000	0.002
$4f_2$	0.011	0.011
12k	0.025	0.042

Subject to the same limitation as for charges, site preferences can be calculated also for the spins carried by the additional electrons. The advantage of the magnetizations is that they can, in principle, be determined fairly easily from experiments – e.g. Mössbauer experiments and total magnetization data led to the proposal that the valence of 2a-Fe changes upon La-doping. Equation (1) shows that due to the half-metallic character the dependence of the total magnetization on x contains no information on such preferences. The calculated DOS shown in Figure 4 confirm, however, that the half-metallic state is due to E_F entering the (global) minority spin DOS. From the projected DOS in Figure 3 it is seen that indeed only 2a-, 2b-, and 12k-Fe contribute to this part of the total DOS. Again we consider the difference of the concentration dependent sublattice magnetizations $m_i(x)$ with respect to the situation in the stoichiometric Sr-hexaferrite:

$$\Delta m_i(x) = m_i(0) - m_i(x). \quad (2)$$

Note the different sign compared to the charge difference. Due to the gap in the total majority spin DOS only the population of the minority spin states is changed and it increases. This implies in the ferrimagnetic arrangement a decreasing absolute sublattice magnetization on 2a-, 2b-, and 12k-sites, but an increasing one on the antiparallel 4f-sublattices.

Figure 6 shows that the redistribution of spins in the unit cell upon doping are, in fact, predicted to be fairly complex. In accord with the charge distributions discussed above there are no changes on the $4f_1$-sublattice and the results for the 2a- and 2b-sites show no systematic dependence on U. Again, the main effect of the on-site repulsion is to increase any preference the system might have for the 12k-sites, and suppressing migration to the $4f_2$-sites. There are differences in the details of the charge and spin redistribution upon doping but a direct comparison of the charge and spin count rests on the assumption that the majority spin states of all individual Fe ions are completely filled and stay so. This may well not be the case with the precision required here to allow a discussion of such details.

5 Conclusions

With the LSDA we found that the stoichiometric strontium ferrite is metallic. Use of the generalized gradient

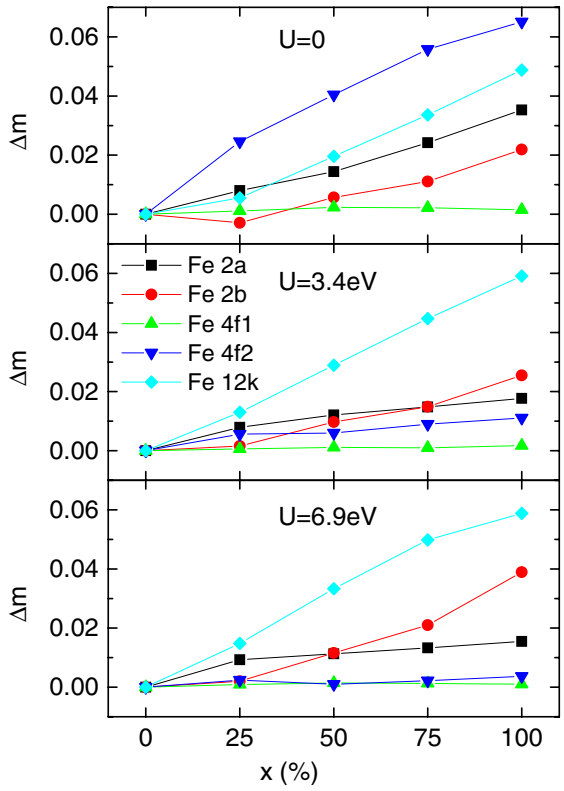

Fig. 6. $\Delta m = m(0) - m(x)$ as function of the La concentration for the GGA (upper panel), GGA+U, $U = 3.4$ eV (middle panel) and $U = 6.9$ eV (lower panel) calculations. Note that due to the definition (Eq. (2)) of Δm the absolute values of sublattice magnetizations on 2a-, 2b-, and 12k decrease while they increase on $4f_1$ and $4f_2$.

approximation (GGA) led to a structure on the border between metal and insulator and only an improved description of the electron correlation (GGA+U method) resulted in an insulating state. All mixed valence compounds including the stoichiometric $LaFe_{12}O_{19}$ are halfmetals with conduction in the minority spin channel. This halfmetal character is consistent with magnetization, conductivity, and NMR experimental data.

The question of site preferences for the additional electrons was addressed by calculating the changes in the charge and spin distribution in the atomic spheres and in the interstitial regime upon La doping. For GGA+U similar results were obtained for both distributions. The overall changes of charge or spin counts in the atomic spheres are small, in contrast to the empirical model of localization at the 2*a* sites. The majority of the electrons introduced by the substitution of Sr by La ends up in the interstitial regime, without clear indications for localization. No change occurs on the $4f_1$-sites, a relatively small increase of the charge is obtained for the 2a-sublattice and app. twice as much on 2b-Fe. The largest changes are predicted for the 12k-sites, but they depend on the on-site Coulomb parameter U, as they do for $4f_2$-Fe. In view of the small absolute changes in the local charge and spin distribution the consistent results obtained in this work lead us to hope that an ab initio calculation of the orbital momentum, the hyperfine fields, and the magnetocrystalline anisotropy might be possible and lead to a consistent understanding of these parameters beyond the simple localization model.

The work was supported by projects 202/03/0552 of the Grant Agency of the Czech Republic and AVOZ-010-914. Two of us (M.K. and M.W.P.) kindly acknowledge support by the Austrian FWF under project P15700 and P16500-N02.

References

1. H. Kojima, *Ferromagnetic Materials*, edited by E.P. Wolfarth (North-Holland, Amsterdam, 1982), Vol. 3
2. F.K. Lotgering, J. Phys. Chem. Solids **35**, 1633 (1974)
3. V.L. Moruzzi, M.W. Shafer, J. Am. Ceramic Soc. **43**, 367 (1960)
4. J.F. Wang, C.B. Ponton, I.R. Harris, J. Magn. Magn. Mater. **234**, 233 (2001)
5. Ch. Sauer, U. Köbler, W. Zinn, J. Phys. Chem. Solids **39**, 1197 (1978)
6. C.M. Fang, F. Kools, R. Metselaar, G. de With, R.A. de Groot, J. Phys.: Condens Matter **15**, 6229 (2003)
7. E.W. Gorter, Proc. IEEE **104B**, 255 (1957)
8. P. Blaha, K. Schwarz, G.K.H. Madsen, D. Kvasnicka, J. Luitz, *WIEN2k, An Augmented PlaneWave + Local Orbitals Program for Calculating Crystal Properties*, Karlheinz Schwarz, Techn. Universtät Wien Austria, 2001. ISBN 3-9501031-1-2
9. V. Adelsköld, Arkiv för Kemi, Mineralogi Och Geologi **12A**, 29 (1938)
10. G. Albanese, J. Phys. Colloq. France **38**, C1-85 (1977)
11. D. Singh, *Plane waves, pseudopotentials and the LAPW method* (Kluwer Academic, 1994)
12. J.P. Perdew, S. Burke, M. Ernzerhof, Phys. Rev. Lett. **77**, 3865 (1996)
13. J.P. Perdew, Y. Wang, Phys. Rev. B **45**, 13 244 (1992)
14. Z. Yang, Z. Huang, L. Ye, X. Xie, Phys. Rev. B **60**, 15674 (1999)
15. A.I. Liechtenstein, V.I. Anisimov, J. Zaanen, Phys. Rev. B **52**, 5467 (1995)
16. I. Solovyev, N. Hamada, K. Terakura, Phys. Rev. B **53**, 7158 (1996)
17. R. Zimmerman, P. Steiner, R. Claessen. F. Reinert, S. Hüfner, P. Blaha, P. Dufek, J. Phys.: Condens. Matter **11**, 1657 (1999)
18. W.E. Pickett, D.J. Singh, Phys. Rev. B **55**, 8642 (1997)
19. P. Novák, F. Boucher, P. Gressier, P. Blaha, K. Schwarz, Phys. Rev. B **63**, 235114 (2001)
20. M.W. Pieper, M. Küpferling, unpublished data
21. M.W. Pieper, M. Küpferling, I.R. Harris, J.F. Wang, J. Mag. Mag. Mat. **272-276**, 2219 (2004)
22. G. Madsen, P. Novák, Europhys. Lett. **69**, 777 (2005)
23. K. Koepernik, B. Velický, R. Hayn, H. Eschrig, Phys. Rev. B **58**, 6944 (1988)
24. R.F.W. Bader, `http://www.chemistry.mcmaster.ca/faculty/bader/aim/`, 2001